A2QTGN: Adaptive Amplitude Quantum-Integrated Temporal Graph Network for Dynamic Link Prediction

Nouhaila Innan[1,2], M. Murali Karthick[3], Simeon Kandan Sonar[3], Vivek Chaturvedi[3], Muhammad Shafique[1,2]
[1]eBRAIN Lab, Division of Engineering, New York University Abu Dhabi (NYUAD), Abu Dhabi, UAE
[2]Center for Quantum and Topological Systems (CQTS), NYUAD Research Institute, NYUAD, Abu Dhabi, UAE
[3]Indian Institute of Technology Palakkad (IITPKD), Palakkad 678623, India
{nouhaila.innan, muhammad.shafique}@nyu.edu, {112301019,112301031}@smail.iitpkd.ac.in, vivek@iitpkd.ac.in

arXiv:2605.21916v1 [quant-ph] 21 May 2026

***Abstract*—Dynamic link prediction is important for modeling evolving interactions in complex systems, including social, communication, financial, and transportation networks. Classical temporal graph models capture sequential dependencies, but they may struggle to represent concurrent and rapidly changing node-edge interactions in large dynamic graphs. We propose A2QTGN (Adaptive Amplitude Quantum-Integrated Temporal Graph Network), a hybrid quantum-classical framework that combines adaptive amplitude encoding with a Temporal Graph Network backbone. The proposed mechanism represents node interaction features as quantum states and selectively refreshes amplitude embeddings based on temporal activity, preserving stable node states while emphasizing meaningful structural changes. This design reduces unnecessary quantum re-encoding and improves temporal representation for link prediction. Experiments on five Temporal Graph Benchmark datasets show that A2QTGN achieves strong predictive and ranking performance across diverse dynamic graphs. Ablation studies confirm the importance of both the quantum embedding module and the adaptive update strategy, while hardware-aware inference using a noisy backend and limited real-device execution supports the feasibility of near-term quantum-assisted temporal graph learning.**

***Index Terms*—Quantum Machine Learning, Temporal Graph Networks, Amplitude Encoding, Dynamic Graphs, Link Prediction**

I. Introduction

Dynamic graphs, which represent systems whose structure changes over time, capture sequences of graph snapshots where both nodes and edges may appear, disappear, or update their attributes [1]. As illustrated in Fig. 1, such representations naturally arise in social platforms, recommender systems, financial transaction ecosystems, and large-scale transportation networks. A central computational challenge in these domains is *dynamic link prediction* [2], the task of forecasting future edge formation or dissolution. Accurate prediction enables critical downstream applications, including friend recommendation, fraud detection, anomaly monitoring, and biological network analysis. Conventional approaches, including static Graph Neural Network (GNN) [3], temporal GNNs, autoregressive sequence models, and heuristic predictors, often struggle to capture long-range temporal dependencies, structural drift, and the non-stationary behaviors characteristic of evolving relational systems [4], [5]. These limitations are further amplified by fairness and bias concerns, as undesirable patterns can accumulate or propagate across successive graph states, ultimately constraining reliable deployment in real-world settings.

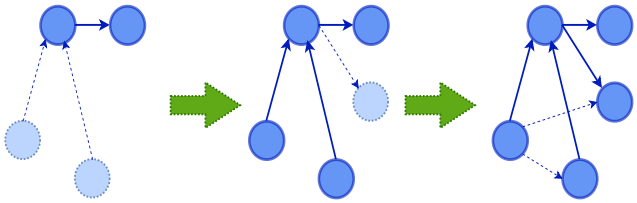

Fig. 1: Dynamic graphs

Recent progress in quantum embedding techniques provides a promising avenue for addressing these gaps [6], [7]. Instead of relying on claims of exponential advantage, quantum-inspired feature maps offer alternative geometric representations by transforming classical inputs into structured quantum states whose inner-product relationships may reveal patterns not easily captured by standard encoders. These embeddings modify the underlying decision boundary in feature space, potentially enabling models to distinguish subtle structural variations in evolving graphs.

Prior hybrid studies have demonstrated that augmenting classical architectures with parametrized quantum circuits can improve representation quality, introduce non-linear feature transformations, and stabilize optimization dynamics [8]–[12]. These observations motivate deeper exploration into quantum-enhanced temporal graph models.

However, most existing quantum–graph approaches remain limited to static scenarios and do not incorporate mechanisms that adapt quantum representations as the graph evolves. This gap highlights the need for quantum embeddings that are both expressive and temporally responsive, enabling effective modeling of continuously changing relational structures.

To address these challenges, we propose the **A2QTGN**, an *Adaptive Amplitude Quantum-Integrated Temporal Graph Network*, that integrates adaptive quantum feature encoding

with a classical Temporal Graph Network (TGN) backbone. The model introduces a selective quantum update mechanism that re-encodes node states only when feature variations exceed a defined activity threshold, efficiently coupling quantum state evolution with temporal memory propagation.

Our main contributions are summarized as follows:

1) We propose **Adaptive Amplitude Encoding (AAE)**, a dynamic quantum embedding mechanism that updates amplitude representations according to temporal feature variations while avoiding unnecessary quantum re-encoding.
2) We design a **hybrid Quantum–TGN pipeline** that combines AAE with a lightweight TGN backbone for end-to-end learning on evolving graph streams without increasing circuit depth with graph size.
3) We introduce an **adaptive quantum update strategy** that determines when quantum embeddings should be refreshed, improving generalization over always-update and no-update variants.
4) We provide a **comprehensive evaluation** on five TGBL link-prediction datasets, including baseline comparisons, ablation studies, convergence analysis, and hardware-aware inference with a limited real-device execution check.

The rest of the paper is organized as follows: **Section II** reviews related work on temporal graph networks, classical link prediction, and quantum approaches. **Section III** details the proposed A2QTGN framework including quantum encoding and temporal memory modules. **Section IV** presents experimental results, performance comparisons, and ablation studies on benchmark datasets. Finally, **Section V** concludes the paper with a summary and discusses future research directions.

II. Related Work

Prior studies on link prediction can be systematically categorized into three major methodological strands: those that capture time-evolving relationships through **temporal graph networks**, those employing established techniques such as **classical link predictors and meta-learning** approaches, and those exploring the potential of quantum computation with **quantum link prediction methods**.

A. Temporal Graph Networks

The evolution of temporal graph networks began with models like JODIE [13], which used recurrent neural networks to model continuous-time dynamics, but its sequential dependency incurred high computational cost and limited scalability. This led to the foundational TGN [14], which introduced an efficient, event-driven message passing mechanism coupled with a node memory module for inductive learning on streaming graphs. However, TGN's design suffered from two primary shortcomings which were limited expressive power due to simple aggregation, and poor generalization across diverse networks. Post-TGN advancements addressed these issues through architectural diversification: TGAT [15] utilized self-attention for better aggregation but faced quadratic complexity; PINT [16] enforced provably injective message passing to enhance expressivity; and lightweight models like GraphMixer [17] favored efficiency using MLPs but often sacrificed performance on complex dynamics. The latest trend, exemplified by research into TGS [18], aims to overcome the generalization barrier by using large-scale pre-training to establish transferable knowledge and neural scaling laws for dynamic graphs.

B. Classical Link Predictors, Embeddings, and Meta-Learning

Link prediction in static and dynamic graphs remains a challenge, as extensively studied by Ghasemian *et al.* [19]. Their evaluation across hundreds of real-world networks demonstrated that no single algorithm dominates, leading to the consensus that near-optimal performance relies on meta-learning ensembles combining multiple structural and embedding-based methods. While models that integrate node attributes, such as AGEE [20], successfully push performance yielding a 3% improvement over conventional embedding methods, the struggle for efficiency and expressivity persists in increasingly complex scenarios. For instance, methods designed for highly expressive knowledge graph link prediction, such as ComplEx [21] or RotatE [22], achieved high scores but are fundamentally constrained by their transductive nature and high computational demands, struggling to scale to the billions of edges found in massive industrial graphs. Similarly, while deep GNN architectures like **GraIL** [23] enable inductive link prediction, they require expensive local sub-graph extraction for every link prediction query, drastically increasing the inference latency and posing a clear, quantitative trade-off between structural expressivity and the necessity of real-time computational efficiency. This ongoing friction necessitates continued research into scalable yet highly expressive models.

C. Quantum Link Prediction and Embeddings

Recent efforts have explored quantum models for link prediction and representation learning. Fundamental to this area are quantum encoding schemes, including basic strategies such as angle encoding [24] and Amplitude encoding [24], as well as more complex circuit-based methods, including Instantaneous Quantum Polynomial (IQP) circuits and Quantum Approximate Optimization Algorithm (QAOA)–inspired circuits, all of which map classical features into expressive quantum states. Building upon these foundational encoding techniques, specialized quantum models have been developed for relational tasks. PQKELP [25], for instance, introduced a projected quantum kernel embedding approach tailored for dynamic networks, demonstrating that quantum feature mappings can significantly improve relational reasoning capabilities. Concurrently, Moutinho *et al.* [26] proposed a quantum-walk-based link prediction model, effectively showing how quantum interference effects can be harnessed to uncover latent connectivity patterns.

Despite these critical advances, existing quantum approaches predominantly operate on static graphs. They fundamentally lack dedicated mechanisms for temporal memory or continuous-

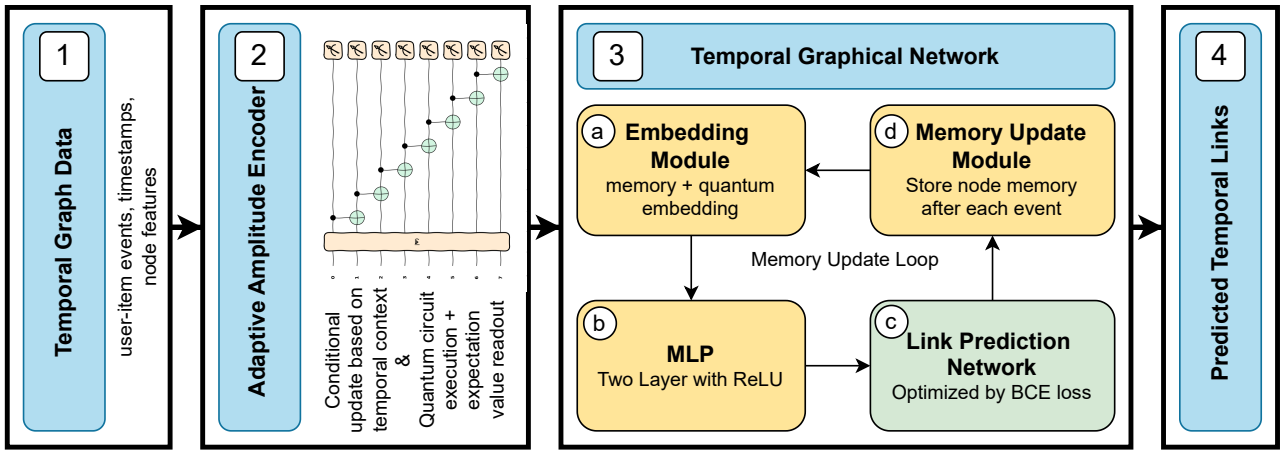

Fig. 2: Pipeline of the A2QTGN methodology. The system processes a temporal interaction stream $\{(u_t, v_t, X_t, F_t, t)\}$ and converts it into future link predictions through four coordinated modules: (a) temporal interaction data forming the discrete-time graph sequence $\mathcal{G}_t = (V_t, E_t, X_t, F_t)$; (b) the AAE, which computes temporal feature variation $\Delta x_{i,t}$, derives the activity factor $\alpha_{i,t} = \sigma(\beta\|\Delta x_{i,t}\|_2)$, and conditionally re-encodes the node into a quantum state $|\psi_{i,t}\rangle$ whose expectation values yield the embedding $z_{i,t}$; (c) the TGN memory mechanism, where node memories $m_{i,t}$ are updated using the fused representation $h_{i,t} = \mathrm{NN}([m_{i,t}^{\mathrm{prev}} \parallel z_{i,t}])$; and (d) the link prediction module, which scores user–item pairs via $\sigma(\mathrm{MLP}([h_{u,t} \parallel h_{i,t}]))$. The diagram depicts these components and their interactions, emphasizing how adaptive quantum encoding and temporal memory propagation jointly support dynamic link prediction.

time node representation, limiting their ability to effectively capture long-term dependencies in evolving graph structures.

To address these gaps, we introduce the **A2QTGN**, which integrates adaptive quantum encoding within a temporal graph framework to enable dynamic node-state modeling and efficient temporal information propagation.

III. Methodology

The proposed framework, **A2QTGN**, integrates quantum feature encoding within a temporal graph learning architecture to enable dynamic link prediction on evolving graphs. The model combines two complementary modules: (1) the *AAE*, which encodes temporal variations of node features into quantum states, and (2) a memory-based *TGN*, which propagates temporal dependencies across events for link prediction.

An overview of the workflow is shown in Fig. 2. Temporal interaction data are processed sequentially: node features are quantum-encoded using the AAE, integrated into temporal embeddings through the TGN memory mechanism, and finally used for link prediction. The following subsections describe each component in detail.

A. Discrete Temporal Graph Formulation

To support the proposed methodology, the temporal learning pipeline first requires a structured representation of how the graph evolves over time. In this work, we adopt a discrete temporal graph formulation that aligns with the event-driven processing of A2QTGN.

A discrete temporal graph is modeled as a sequence of graph snapshots indexed by discrete time steps:

$$\mathcal{G} = \{\mathbf{G}_t = (\mathbf{V}_t, \mathbf{E}_t, \mathbf{X}_t, \mathbf{F}_t)\}_{t=1}^{T}, \tag{1}$$

where $\mathbf{V}_t$ denotes the set of nodes at time t, $\mathbf{E}_t \subseteq \mathbf{V}_t \times \mathbf{V}_t$ is the set of observed edges, $\mathbf{X}_t$ represents the node feature matrix, and $\mathbf{F}_t$ represents the corresponding edge feature matrix. Each incoming interaction event, typically a user–item pair (u, v) at time t, updates the graph with temporally varying features encoded in $\mathbf{X}_t$ and $\mathbf{F}_t$.

The dynamic link prediction objective is to infer future interactions by using all historical snapshots up to time t. Formally, given $\{\mathbf{G}_\tau\}_{\tau \le t}$, the model learns a mapping

$$f : \{\mathbf{G}_1, \ldots, \mathbf{G}_t\} \to \mathbb{P}((u, v, f_{uv}) \in \mathbf{E}_{t'}), \quad t' > t, \tag{2}$$

which estimates the probability that an edge (u, v) with attributes f_{uv} will appear at a future time t'. This formulation ensures that both structural evolution and temporal variations in node and edge features are explicitly captured, forming the foundation for the quantum–temporal processing pipeline of A2QTGN.

B. Adaptive Amplitude Encoding

The AAE module represents the core novelty of our approach, addressing a fundamental efficiency challenge in temporal quantum graph processing. This module efficiently translates changes in node features over time into the quantum amplitude space. Rather than re-encoding every node at every timestep, AAE measures the magnitude of feature change and adjusts the encoding accordingly. Nodes that exhibit meaningful temporal variation receive fresh amplitude embeddings, while nodes with minimal change simply retain their previous quantum state. This adaptive mechanism allows the model to focus computational effort where the graph is evolving most, significantly improving efficiency while preserving the expressiveness of the learned representations.

In the implemented circuit (see Fig. 2-AAE), $x'_{i,t}$ is normalized and encoded via `AmplitudeEmbedding` [27], with pairwise entanglement introduced using a sequence of

Algorithm 1 AAE

Require: Temporal graph $\{G_t = (V_t, E_t, X_t)\}_{t=1}^{T}$, TGN model f_{TGN}, threshold τ

Initialize encoded states $\{|\psi_{i,1}\rangle\}$ from $X_{i,1}$
for each time step $t = 2$ to T **do**
  for each node $v_i \in V_t$ **do**
    Compute temporal change: $\Delta x_{i,t} = X_{i,t} - X_{i,t-1}$
    Calculate activity factor: $\alpha_{i,t} = \sigma(\beta \|\Delta x_{i,t}\|)$
    if $\alpha_{i,t} > \tau$ **then**
      Update amplitude vector: $x'_{i,t} = \frac{X_{i,t-1} + \alpha_{i,t}\Delta x_{i,t}}{\|X_{i,t-1} + \alpha_{i,t}\Delta x_{i,t}\|}$
      Encode $x'_{i,t} \to |\psi_{i,t}\rangle$
    else
      Reuse previous state: $|\psi_{i,t}\rangle = |\psi_{i,t-1}\rangle$
    end if
    Obtain quantum embedding: $z_{i,t} = \langle\psi_{i,t}|H|\psi_{i,t}\rangle$
  end for
  Update temporal graph representation: $h_t = f_{\text{TGN}}(\{z_{i,t}\}, E_t)$
  Compute link prediction loss $\mathcal{L}_t$
end for

controlled-NOT gates. The expectation values of the Pauli-Z operators form the quantum embedding vector $z_{i,t}$. This vector reflects both the current feature magnitude and the temporal change intensity modulated by $\alpha_{i,t}$, allowing the network to differentiate between rapid and slow evolving nodes.

C. Temporal Memory Update

The temporal memory update module is responsible for tracking historical dynamics and maintaining a long-term profile for each node (users and items). It builds on the core principles of the TGN architecture. Specifically, TGN introduces a continuous-time memory mechanism in which each node maintains a dedicated memory vector that is updated only when new interaction events occur. This event-driven paradigm enables efficient processing of large-scale temporal graphs without recomputing entire node histories at every time step.

In our framework, this principle is adopted by assigning every user and item a persistent memory state m_i together with an associated timestamp t_{last}. When a new interaction involving node i is observed at time t, its memory is retrieved and combined with the freshly generated quantum-temporal embedding $z_{i,t}$ to produce an updated node representation. The resulting high-dimensional embedding $h_{i,t}$ is then written back into the node's memory, mirroring TGN's message-based memory update rule. By decoupling the persistent memory (long-term state) from the transient embedding (task-specific state), the module preserves the temporal evolution of each node while enabling efficient real-time adaptation, consistent with the design principles of TGN.

a) ***Memory Storage****:* Each node i maintains a dedicated memory vector $m_i \in \mathbb{R}^{D_{\text{mem}}}$, and a record of the last time it was updated, t_{last}. These are managed by the `MemoryModule` (i.e., `self.user_mem` and `self.item_mem`): The memory state m_i encapsulates the node's long-term history and evolving behavioral patterns.

b) ***Temporal Integration****:* When a new interaction occurs at time t, the node's current memory $m_{i,t_{\text{prev}}}$ is retrieved. This memory is then used, along with the newly computed quantum-encoded feature representation $z_{i,t}$ (derived from the AAE), to calculate a new, high-dimensional temporal embedding $h_{i,t}$:

$$h_{i,t} = \text{EmbeddingModule}(m_{i,t_{\text{prev}}} \parallel z_{i,t}). \tag{3}$$

After $h_{i,t}$ is used for the link prediction task, it is immediately used to update the memory. The new memory state $m_{i,t}$ is set to the current temporal embedding (detached from the computation graph to prevent gradients from flowing backward through time), and the update timestamp is set to t:

$$m_{i,t} \leftarrow h_{i,t}, \quad t_{\text{last}} \leftarrow t.$$

This process ensures that the memory is incrementally updated in real-time with the most recent, relevant temporal information, allowing the model to adapt its predictions dynamically.

D. Node Representation and Link Prediction:

The formation of the node-level embedding and its subsequent use for link prediction is a two-step process, combining adaptive quantum encoding with a classical neural network for final representation and scoring.

a) ***Adaptive Quantum Encoding*** *($x \to z$):* The AAE is used to create an intermediate quantum-derived feature $z_{i,t}$ for a node i based on the change in its features between interactions.

1) **Change Detection:** The temporal feature change $\Delta x_{i,t}$ is computed: $\Delta x_{i,t} = X_{\text{curr}} - X_{\text{prev}}$.
2) **Activity Factor:** An activity factor α is calculated using a sigmoid function σ applied to the ℓ_2-norm of the change, weighted by a hyperparameter β: $\alpha = \sigma(\beta\|\Delta x_{i,t}\|)$.
3) **Adaptive Update (x'):** The encoder checks if α exceeds a threshold τ. If the change is significant ($\alpha > \tau$), a new feature vector is calculated as $X_{\text{prev}} + \alpha\Delta x_{i,t}$ and normalized to form x'. If the change is insignificant, the previous state X_{prev} is retained. This ensures only salient temporal changes are propagated, reducing the encoding of noise.
4) **Quantum Embedding (z):** The vector x' is then padded and encoded into a quantum state $|\psi\rangle$ using `qml.AmplitudeEmbedding`. The intermediate feature z is then extracted by measuring the expectation value of Pauli-Z operators ($\hat{Z}$) on all qubits: $z = \left(\langle\psi|\hat{Z}_1|\psi\rangle, \ldots, \langle\psi|\hat{Z}_{N_{\text{qubit}}}|\psi\rangle\right)$.

b) ***Node Embedding Formation*** *($z \to h$):* The final node-level temporal embedding $h_{i,t}$ is generated by the `EmbeddingModule`. This module acts as a feature fusion layer, concatenating the node's long-term memory $m_{i,t_{\text{prev}}}$ with the freshly generated quantum-encoded feature $z_{i,t}$: $h_{i,t} = \text{NN}([m_{i,t_{\text{prev}}} \parallel z_{i,t}])$ This process creates a comprehensive node representation that captures both the long-term history (via m) and the immediate, relevant quantum-compressed temporal change (via z).

*c) **Link Prediction**:* For a given potential interaction between a user u and an item i, their respective final temporal embeddings $h_{u,t}$ and $h_{i,t}$ are obtained. These two embeddings are concatenated and passed through a scoring Multi-Layer Perceptron (MLP), denoted as Scorer, followed by a sigmoid activation σ:

$$P(\text{Link}) = \sigma(\text{Scorer}([h_{u,t} \parallel h_{i,t}])). \tag{4}$$

The output is a scalar score representing the probability of a link forming, which is optimized against the ground truth labels using Binary Cross-Entropy (BCE) loss during training.

The overall end-to-end workflow is summarized in Algorithm 1, which iterates through temporal interactions, performs adaptive quantum encoding, updates node memories through the TGN backbone, and optimizes the binary cross-entropy loss for link prediction.

Algorithm 2 Quantum Temporal Graph Network

Require: Temporal graph $\{G_t = (V_t, E_t, X_t)\}_{t=1}^{T}$, memory modules, AAE (Algorithm 1)
Ensure: Link prediction probability $P(\text{Link})$
for $t = 1$ to T **do** ▷ Iterate over time
Node Processing
  for each node $i \in V_t$ **do**
    $z_{i,t} \leftarrow \text{AAE}(X_{i,t}, X_{i,t-1})$ ▷ Compute quantum embedding using Algorithm 1
    $m_{i,t_{\text{prev}}} \leftarrow \text{mem.get}(i)$ ▷ Retrieve previous memory
    $h_{i,t} \leftarrow \text{EmbeddingModule}(m_{i,t_{\text{prev}}} \parallel z_{i,t})$ ▷ Fuse memory and quantum features
  end for
Edge Processing
  for each interaction $(u, i) \in E_t$ **do**
    $P_{u,i,t} \leftarrow \sigma(\text{Scorer}(h_{u,t} \parallel h_{i,t}))$ ▷ Predict link probability
  end for
Memory Update
  for each node $i \in V_t$ **do**
    $\text{mem.update}(i, h_{i,t}, t)$ ▷ Store updated memory
  end for
  $\mathcal{L}_t \leftarrow \text{BCE}(P_t^+, 1) + \text{BCE}(P_t^-, 0)$ ▷ Compute loss
end for
return $P(\text{Link})$

IV. Results and Discussion

A. Experimental Setup

We evaluate the proposed A2QTGN framework on five temporal link-prediction benchmark datasets from the Temporal Graph Benchmark Suite: `tgbl-wiki`, `tgbl-review`, `tgbl-coin`, `tgbl- comment`, and `tgbl- flight` [28]. Their approximate statistics are shown in Table I.

The dataset follows the standard link-prediction setup with a temporal split of 70% for training, 15% for validation, and 15% for testing. Negative samples are generated by pairing each positive interaction with an item the user has not previously interacted with. The model uses eight qubits, a 64-dimensional memory, and a 64-dimensional output embedding, and is trained with the Adam optimizer at a learning rate of 1e-3 and a batch size of 32.

TABLE I: Statistics of the TGBL datasets used for evaluation.

Dataset	# Nodes	# Edges
`tgbl-wiki`	9,227	157,474
`tgbl-review`	352,637	4,873,540
`tgbl-coin`	638,486	22,809,486
`tgbl-comment`	994,790	44,314,507
`tgbl-flight`	18,143	67,169,570

The main simulation experiments are conducted using the PennyLane `lightning.qubit`. For hardware-aware inference, we further evaluate the trained model using the IBM `ibm_torino` quantum device under a constrained 100-shot setting and the corresponding `FakeTorino` noisy backend with 2048 shots. Evaluation is conducted using accuracy, precision, AUC, and Mean Reciprocal Rank (MRR). MRR assesses ranking quality by measuring how highly the first correct prediction appears in the ranked output. For a set of queries Q, it is computed as:

$$\text{MRR} = \frac{1}{|Q|} \sum_{i=1}^{|Q|} \frac{1}{\text{rank}_i}, \tag{5}$$

where rank_i denotes the rank position of the first relevant item for the i-th query.

B. Performance Analysis

The objective of this experiment is to evaluate how effectively A2QTGN models temporal interactions and predicts future links across diverse real-world dynamic graphs. Table II reports the train, validation, and test performance of A2QTGN on the five TGBL datasets using accuracy, precision, AUC, and MRR. A2QTGN achieves strong performance across the evaluated temporal graph datasets, with test AUC values ranging from 0.7657 on `tgbl-review` to 0.9957 on `tgbl-flight`. The model performs particularly well on `tgbl-wiki` and `tgbl-flight`, reaching test accuracies of 93.03% and 97.83%, respectively. In terms of ranking quality, A2QTGN obtains the highest test MRR on `tgbl-flight` with 0.7832, followed closely by `tgbl-wiki` with 0.7782.

TABLE II: Train, validation, and test performance of A2QTGN on TGBL datasets.

Split	Metric	Wiki	Review	Coin	Comment	Flight
Train	Accuracy	92.72%	71.13%	73.66%	81.40%	96.67%
	Precision	90.49%	76.81%	85.25%	82.81%	95.31%
	AUC	0.9809	0.7665	0.8050	0.8842	0.9921
	MRR	0.7651	0.5732	0.6125	0.6642	0.7811
Validation	Accuracy	92.99%	68.69%	78.61%	80.63%	97.35%
	Precision	90.25%	69.41%	80.21%	77.84%	95.33%
	AUC	0.9845	0.7921	0.8784	0.8817	0.9922
	MRR	0.7674	0.6142	0.6624	0.6409	0.7808
Test	Accuracy	93.03%	64.99%	79.87%	79.67%	97.83%
	Precision	90.13%	65.76%	80.97%	77.48%	96.07%
	AUC	0.9857	0.7657	0.8886	0.8725	0.9957
	MRR	0.7782	0.5883	0.6668	0.6383	0.7832

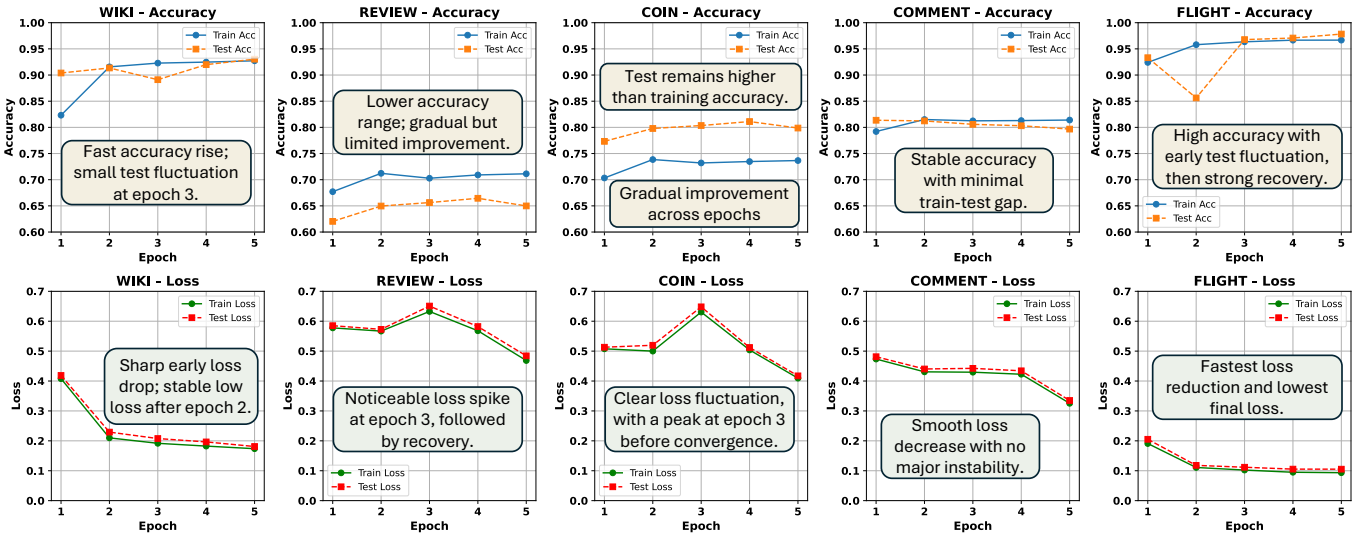

Fig. 3: Performance convergence on various datasets.

These results indicate that A2QTGN can capture predictive temporal interaction patterns across datasets with different structural and temporal properties.

The results also reveal dataset-dependent behavior. The strongest overall predictive performance is observed on `tgbl-flight`, where the model achieves 97.83% accuracy, 96.07% precision, 0.9957 AUC, and 0.7832 MRR on the test split. This suggests that the temporal interaction patterns in this dataset are highly learnable by the proposed adaptive quantum-temporal architecture. In contrast, `tgbl-review` is the most challenging dataset, with a test accuracy of 64.99%, precision of 65.76%, AUC of 0.7657, and MRR of 0.5883. This may reflect weaker temporal regularity, higher interaction variability, or less predictable link formation patterns.

Across train, validation, and test splits, A2QTGN remains stable on `tgbl-wiki`, `tgbl-comment`, and `tgbl-flight`. For example, `tgbl-flight` improves from 96.67% training accuracy to 97.83% test accuracy, while its MRR remains nearly unchanged across the three splits. Similarly, `tgbl-wiki` remains consistently above 92% accuracy and maintains stable MRR values from training to testing. For `tgbl-review`, the lower validation and test scores indicate a more difficult generalization setting. Meanwhile, `tgbl-coin` shows an increase in AUC from 0.8050 during training to 0.8886 on the test split, with MRR also increasing from 0.6125 to 0.6668, suggesting that the learned representation remains effective beyond the training period.

C. Algorithmic Convergence Performance

The objective of this experiment is to evaluate the convergence speed and stability of A2QTGN during training across graphs of varying scales. As shown in Fig. 3, A2QTGN exhibits stable convergence behavior across the evaluated datasets. The model converges rapidly on `tgbl-wiki` and maintains smooth learning trends on larger graphs such as `tgbl-coin`. The training and validation curves remain relatively close throughout training, suggesting that the model does not show severe overfitting under the considered settings.

These convergence patterns are consistent with the design of the adaptive update mechanism. By updating the quantum embedding selectively rather than at every time step, A2QTGN can focus quantum encoding updates on more informative temporal changes while avoiding unnecessary recomputation. This selective update strategy helps maintain stable optimization behavior while reducing redundant quantum embedding evaluations.

D. Ablation Study

The ablation study evaluates the contribution of the two main components of A2QTGN: the quantum embedding module and the adaptive quantum embedding update mechanism. We consider three update strategies. First, the proposed adaptive update strategy recomputes the quantum embedding only when the adaptive decision rule is activated. Second, the always-update variant removes the adaptive decision rule and recomputes the quantum embedding at every time step. Third, the no-update baseline disables quantum embedding updates entirely and reuses a fixed embedding throughout the temporal sequence. This design allows us to separate the benefit of using quantum embeddings from the benefit of updating them conditionally. Table III reports the main ablation results on the tgbl-wiki dataset. Removing the quantum embedding module leads to a large performance drop across all metrics, with AUC decreasing from 0.9857 to 0.6014 and MRR decreasing from 0.7782 to 0.2187. This indicates that the proposed quantum embedding provides a more informative temporal representation

TABLE III: Main ablation results on the tgbl-wiki dataset.

Model Variant	Accuracy	Precision	AUC	MRR
A2QTGN	93.03%	90.13%	0.9857	0.7782
w/o Quantum Embedding	54.12%	52.91%	0.6014	0.2187
Always Update	68.47%	67.20%	0.7258	0.3421

in this setting. The always-update variant also shows a clear degradation, reaching 68.47% accuracy, 0.7258 AUC, and 0.3421 MRR. Since this variant still recomputes the quantum embedding but removes the conditional update rule, the result suggests that updating the embedding at every time step is less effective than applying updates selectively.

To further isolate the effect of conditional updating under different data scales, additional experiments are conducted on 10k and 25k subsets of the tgbl-wiki dataset, as reported in Tables IV and V. These experiments compare the proposed adaptive update strategy against the always-update and no-update variants. Across both subsets, A2QTGN consistently achieves the best validation and test performance across accuracy, precision, AUC, and MRR. On the 25k test split, the adaptive model obtains 90.63% accuracy, 89.05% precision, 0.9739 AUC, and 0.7597 MRR. In comparison, the always-update variant reaches 77.27% accuracy, 75.35% precision, 0.8606 AUC, and 0.6458 MRR, while the no-update baseline obtains 68.19% accuracy, 74.60% precision, 0.7479 AUC, and 0.6203 MRR. This corresponds to a test-accuracy gain of 13.36 percentage points over always updating and 22.44 percentage points over the no-update baseline. In terms of MRR, the adaptive model improves over the always-update and no-update variants by 0.1139 and 0.1394, respectively.

TABLE IV: Update-strategy ablation on the 10k subset of the tgbl-wiki dataset.

Split	Update Strategy	Accuracy	Precision	AUC	MRR
Train	Adaptive Update	91.71%	88.74%	0.9759	0.7583
	Always Update	83.95%	81.56%	0.9166	0.6912
	No Update	83.51%	82.57%	0.9134	0.6943
Val	Adaptive Update	92.07%	89.03%	0.9773	0.7678
	Always Update	81.50%	83.99%	0.9067	0.6915
	No Update	70.13%	79.94%	0.7909	0.6809
Test	Adaptive Update	92.52%	89.17%	0.9798	0.7782
	Always Update	80.28%	83.80%	0.8955	0.6877
	No Update	68.79%	80.63%	0.7528	0.6351

TABLE V: Update-strategy ablation on the 25k subset of the tgbl-wiki dataset.

Split	Update Strategy	Accuracy	Precision	AUC	MRR
Train	Adaptive Update	91.21%	88.56%	0.9751	0.7704
	Always Update	81.43%	80.82%	0.9012	0.6735
	No Update	86.72%	87.71%	0.9391	0.7282
Val	Adaptive Update	92.09%	90.44%	0.9783	0.7693
	Always Update	78.61%	76.39%	0.8865	0.6671
	No Update	67.53%	78.65%	0.7767	0.6231
Test	Adaptive Update	90.63%	89.05%	0.9739	0.7597
	Always Update	77.27%	75.35%	0.8606	0.6458
	No Update	68.19%	74.60%	0.7479	0.6203

E. Comparative Analysis

We further conduct a two-level comparative analysis to evaluate A2QTGN from both a quantum-encoding perspective and a broader temporal graph learning perspective.

(1) Intra-quantum comparison: We first compare several quantum embedding strategies integrated with the same TGN backbone, including angle embedding, amplitude embedding, IQP embedding, and QAOA-based embedding, as reported in Table VI. This comparison isolates the impact of the quantum feature encoding strategy while keeping the temporal graph backbone fixed. Among the quantum-only baselines, amplitude embedding achieves the strongest overall performance, reaching 74.96% accuracy and 0.8056 AUC, while angle and QAOA embeddings provide moderate improvements over the classical TGN baseline. IQP embedding shows limited performance in this setting, suggesting that its representation may be less effective for the temporal relational patterns in `tgbl-wiki`. In contrast, A2QTGN achieves the best results across all metrics, with 93.03% accuracy, 90.13% precision, 0.9857 AUC, and 0.7782 MRR. These results indicate that the gain does not come only from inserting a quantum embedding into TGN, but from combining quantum-enhanced representations with the proposed adaptive temporal update mechanism.

TABLE VI: Model performance comparison on the tgbl-wiki dataset.

Model	Accuracy	Precision	AUC	MRR
Angle Emb + TGN	65.91%	39.59%	0.7086	0.3438
Amplitude Emb + TGN	74.96%	46.00%	0.8056	0.3199
IQP Emb + TGN	49.73%	23.67%	0.5349	0.1638
QAOA Emb + TGN	68.04%	34.68%	0.7313	0.2828
TGN	43.82%	18.30%	0.4710	0.1748
A2QTGN (Ours)	**93.03%**	**90.13%**	**0.9857**	**0.7782**

(2) Model-level comparison: We next compare A2QTGN with representative temporal graph learning baselines across multiple TGBL datasets using MRR, as reported in Table VII. The comparison includes EdgeBank, DyRep, TGN, CAWN, NAT, DyGFormer, and TGAT, with baseline values taken from prior TGBL evaluations. The symbol "–" denotes cases where the corresponding baseline could not be evaluated on the given dataset under the same setting due to scalability and computational constraints.

A2QTGN achieves strong ranking performance across the evaluated datasets. It obtains the best reported MRR on `tgbl-review` and `tgbl-flight`, while remaining competitive on `tgbl-wiki`, `tgbl-coin`, and `tgbl-comment`. On `tgbl-wiki`, DyGFormer reports the highest MRR of 0.798, while A2QTGN achieves 0.7782. On `tgbl-coin`, DyGFormer reaches 0.752, while A2QTGN obtains 0.6688 and improves over EdgeBank, DyRep, and TGN. On `tgbl-comment`, A2QTGN reaches 0.6383, close to DyGFormer at 0.670 and higher than the other reported baselines. On `tgbl-flight`, A2QTGN achieves the highest reported MRR of 0.7832, improving over TGN at 0.705. These results show that A2QTGN provides stable ranking performance across different temporal graph datasets, with the strongest relative gains observed on `tgbl-review` and `tgbl-flight`.

F. Hardware Inference Evaluation

To assess the feasibility of quantum-assisted inference under hardware-aware conditions, we evaluate A2QTGN using the `FakeTorino` backend with 2048 shots. This backend provides a noisy simulation based on the topology and noise model of the corresponding IBM quantum device, allowing controlled and repeatable inference experiments while accounting for realistic quantum noise effects. Unlike ideal statevector simulation, this setting introduces finite-shot estimation and

TABLE VII: MRR performance across TGBL dataset.

Model	Edgebank (tw) [29]	Edgebank (un) [29]	DyRep [30]	TGN [14]	CAWN [31]	NAT [32]	DyGFormer [29]	TGAT [33]	**A2QTGN (Ours)**
tgbl-wiki	0.571	0.495	0.050	0.396	0.711	0.749	0.798	0.141	**0.7782**
tgbl-review	0.025	0.023	0.220	0.349	0.193	0.341	0.224	0.355	**0.5883**
tgbl-coin	0.580	0.359	0.452	0.586	-	-	0.752	-	**0.6688**
tgbl-comment	0.149	0.129	0.289	0.379	-	-	0.670	-	**0.6383**
tgbl-flight	0.387	0.167	0.556	0.705	-	-	-	-	**0.7832**

backend noise, making it suitable for evaluating whether the learned quantum representations remain usable under practical execution constraints. In addition to the `FakeTorino` noisy-backend evaluation, we also execute A2QTGN on an actual IBM quantum device under a constrained 100-shot setting. Since this real-device run uses a small measurement budget, it is reported only as supporting evidence rather than as the main hardware benchmark.

TABLE VIII: Hardware-aware inference performance on the `FakeTorino` backend using 2048 shots and 100 evaluation samples.

Metric	Wiki	Review	Coin	Comment	Flight
Accuracy	86.50%	67.00%	77.00%	73.50%	80.00%
Precision	91.95%	77.00%	73.68%	70.00%	94.12%
AUC	0.9631	0.7676	0.8586	0.7222	0.9654
MRR	0.9778	0.8895	0.9154	0.8226	0.9844

Table VIII reports the main hardware-aware inference results using 100 evaluation samples. A2QTGN maintains strong performance on several datasets despite noisy quantum execution. On `tgbl-wiki`, the model achieves 86.50% accuracy, 91.95% precision, 0.9631 AUC, and 0.9778 MRR. Similarly, `tgbl-flight` reaches 80.00% accuracy, 94.12% precision, 0.9654 AUC, and 0.9844 MRR, indicating that the model preserves strong ranking quality under noisy-backend inference. The `tgbl-coin` dataset also shows stable ranking performance, with an MRR of 0.9154.

The limited real-hardware run further supports executable feasibility under actual device constraints. Despite the restricted 100-shot budget, A2QTGN achieves promising results on selected datasets, including 90.00% accuracy and 1.00 AUC on `tgbl-coin`, as well as 70.00% accuracy and 0.80 AUC on `tgbl-review`. These values should be interpreted cautiously because low-shot execution can introduce high variance, especially in precision and AUC estimates. Nevertheless, they indicate that the learned quantum representations can retain useful predictive behavior even under constrained real-device inference.

The lower results on `tgbl-review` and `tgbl-comment` in the `FakeTorino` backend setting suggest that the effect of hardware-aware noise is dataset dependent. This variation may be related to differences in temporal regularity, class separability, and the sensitivity of the learned quantum embedding to finite-shot measurement noise. A smaller 10-sample noisy-backend evaluation was also performed as an initial feasibility check and showed similar qualitative behavior, but the 100-sample setting is used as the main reported result because it provides a more stable estimate of noisy-backend inference performance.

G. Discussion

The results provide three main insights into the behavior of A2QTGN. First, the model shows strong predictive and ranking performance across datasets with different temporal structures, but the source of difficulty differs by dataset. For example, `tgbl-flight` achieves the highest accuracy and AUC, suggesting that its temporal interaction patterns are highly learnable despite its large edge volume. In contrast, `tgbl-review` presents a more difficult generalization setting, with lower accuracy, precision, AUC, and MRR. This indicates that dataset difficulty is not determined only by graph size, but also by temporal regularity, interaction variability, and the predictability of future links.

Second, the ablation results confirm that both the quantum embedding and the adaptive update rule are important to the final performance. Removing the quantum embedding substantially weakens the representation, while replacing the adaptive rule with always-update or no-update strategies reduces generalization. This suggests that the benefit of A2QTGN does not come only from adding a quantum layer to TGN, but from controlling when quantum representations are refreshed. Selective updating appears to preserve useful temporal information while reducing unnecessary recomputation and limiting unstable representation changes.

Third, the hardware-aware inference results show that the learned quantum representations remain usable under noisy quantum execution. The `FakeTorino` backend results indicate that A2QTGN can preserve strong ranking behavior under finite-shot noisy simulation, especially on `tgbl-wiki`, `tgbl-coin`, and `tgbl-flight`. The limited real-hardware run further supports executable feasibility, although its results should be interpreted cautiously because of the restricted 100-shot budget. These findings suggest that the proposed architecture is compatible with near-term quantum execution, while also showing that performance remains sensitive to shot budget, backend noise, and dataset-specific separability.

Despite these strengths, several limitations remain. The adaptive threshold introduces a trade-off between responsiveness and computational savings: conservative thresholds may miss meaningful temporal changes, while aggressive thresholds may trigger excessive quantum updates. In addition, the quantum embedding capacity may become limiting for high-dimensional or highly heterogeneous temporal graphs unless paired with more effective feature compression or more efficient circuit designs. Future work should therefore study threshold selection, circuit scaling, and hardware-aware optimization strategies to improve robustness on larger and more irregular dynamic graphs.

V. Conclusion

This work presented A2QTGN, a hybrid quantum–classical framework for temporal link prediction that combines adaptive amplitude encoding with a Temporal Graph Network backbone. The proposed design enables quantum embeddings to be updated selectively based on temporal feature changes, reducing redundant re-encoding while preserving informative node-state evolution.

Evaluation on five TGBL datasets shows that A2QTGN achieves strong predictive and ranking performance across diverse dynamic graphs. The results also show that the adaptive update mechanism improves generalization compared with always-update and no-update alternatives, while hardware-aware inference supports the feasibility of executing the model under noisy quantum settings.

Future work will focus on improving scalability for larger and more heterogeneous temporal graphs, refining the adaptive threshold selection, and developing more hardware-efficient quantum circuits for dynamic network analysis.

Acknowledgment

This work was supported in part by the NYUAD Center for Quantum and Topological Systems (CQTS), funded by Tamkeen under the NYUAD Research Institute grant CG008.

References

[1] D. Šiljak, "Dynamic graphs," *Nonlinear Analysis: Hybrid Systems*, vol. 2, no. 2, pp. 544–567, 2008.

[2] F. Poursafaei, S. Huang, K. Pelrine, and R. Rabbany, "Towards better evaluation for dynamic link prediction," *Advances in Neural Information Processing Systems*, vol. 35, pp. 32 928–32 941, 2022.

[3] Z. Wu, S. Pan, F. Chen, G. Long, C. Zhang, and P. S. Yu, "A comprehensive survey on graph neural networks," *IEEE Transactions on Neural Networks and Learning Systems*, vol. 32, no. 1, pp. 4–24, 2021.

[4] S. M. Kazemi, R. Goel, K. Jain, I. Kobyzev, A. Sethi, P. Forsyth, and P. Poupart, "Representation learning for dynamic graphs: A survey," *Journal of Machine Learning Research*, vol. 21, no. 70, pp. 1–73, 2020.

[5] J. Skarding, B. Gabrys, and K. Musial, "Foundations and modeling of dynamic networks using dynamic graph neural networks: A survey," *iEEE Access*, vol. 9, pp. 79 143–79 168, 2021.

[6] S. Lloyd, M. Schuld, A. Ijaz, J. Izaac, and N. Killoran, "Quantum embeddings for machine learning," *arXiv preprint arXiv:2001.03622*, 2020.

[7] N. Innan, A. Rosato, A. Marchisio, and M. Shafique, "How embeddings shape graph neural networks: Classical vs quantum-oriented node representations," *arXiv preprint arXiv:2604.15273*, 2026.

[8] M. Schuld and N. Killoran, "Quantum machine learning in feature hilbert spaces," *Physical review letters*, vol. 122, no. 4, p. 040504, 2019.

[9] V. Havlíček, A. D. Córcoles, K. Temme, A. W. Harrow, A. Kandala, J. M. Chow, and J. M. Gambetta, "Supervised learning with quantum-enhanced feature spaces," *Nature*, vol. 567, no. 7747, pp. 209–212, 2019.

[10] S. Xu, F. Wilhelm-Mauch, and W. Maass, "Quantum feature embeddings for graph neural networks." in *HICSS*, 2024, pp. 7633–7642.

[11] N. Innan, A. Sawaika, A. Dhor, S. Dutta, S. Thota, H. Gokal, N. Patel, M. A.-Z. Khan, I. Theodonis, and M. Bennai, "Financial fraud detection using quantum graph neural networks," *Quantum Machine Intelligence*, vol. 6, no. 1, p. 7, 2024.

[12] N. Innan, R. V. W. Putra, and M. Shafique, "Spate: Spiking-phase adaptive temporal encoding for quantum machine learning," *arXiv preprint arXiv:2604.11022*, 2026.

[13] S. Kumar, X. Zhang, and J. Leskovec, "Predicting dynamic embedding trajectory in temporal interaction networks," in *Proceedings of the 25th ACM SIGKDD International Conference on Knowledge Discovery & Data Mining*, ser. KDD '19. New York, NY, USA: Association for Computing Machinery, 2019, p. 1269–1278. [Online]. Available: https://doi.org/10.1145/3292500.3330895

[14] E. Rossi, B. Chamberlain, F. Frasca, D. Eynard, F. Monti, and M. M. Bronstein, "Temporal graph networks for deep learning on dynamic graphs," *CoRR*, vol. abs/2006.10637, 2020. [Online]. Available: https://arxiv.org/abs/2006.10637

[15] D. Xu, C. Ruan, E. Korpeoglu, S. Kumar, and K. Achan, "Inductive representation learning on temporal graphs," 2020. [Online]. Available: https://arxiv.org/abs/2002.07962

[16] A. H. Souza, D. Mesquita, S. Kaski, and V. Garg, "Provably expressive temporal graph networks," 2022. [Online]. Available: https://arxiv.org/abs/2209.15059

[17] W. Cong, S. Zhang, J. Kang, B. Yuan, H. Wu, X. Zhou, H. Tong, and M. Mahdavi, "Do we really need complicated model architectures for temporal networks?" 2023. [Online]. Available: https://arxiv.org/abs/2302.11636

[18] K. Shamsi, T. G. B. Ngo, R. Shirzadkhani, S. Huang, F. Poursafaei, P. Azad, R. Rabbany, B. Coskunuzer, G. Rabusseau, and C. G. Akcora, "Mint: Multi-network training for transfer learning on temporal graphs," 2025. [Online]. Available: https://arxiv.org/abs/2406.10426

[19] A. Ghasemian, H. Hosseinmardi, A. Galstyan, E. M. Airoldi, and A. Clauset, "Stacking models for nearly optimal link prediction in complex networks," *Proceedings of the National Academy of Sciences*, vol. 117, no. 38, pp. 23 393–23 400, 2020.

[20] W. Gu, J. Hou, and W. Gu, "Improving link prediction accuracy of network embedding algorithms via rich node attribute information," *Journal of Social Computing*, vol. 4, no. 4, p. 326–336, Dec. 2023. [Online]. Available: http://dx.doi.org/10.23919/JSC.2023.0018

[21] T. Trouillon, J. Welbl, S. Riedel, Éric Gaussier, and G. Bouchard, "Complex embeddings for simple link prediction," 2016. [Online]. Available: https://arxiv.org/abs/1606.06357

[22] Z. Sun, Z.-H. Deng, J.-Y. Nie, and J. Tang, "Rotate: Knowledge graph embedding by relational rotation in complex space," 2019. [Online]. Available: https://arxiv.org/abs/1902.10197

[23] K. K. Teru, E. Denis, and W. L. Hamilton, "Inductive relation prediction by subgraph reasoning," 2020. [Online]. Available: https://arxiv.org/abs/1911.06962

[24] A. Tudisco, A. Marchesin, M. Zamboni, M. Graziano, and G. Turvani, "Evaluating angle and amplitude encoding strategies for variational quantum machine learning: their impact on model's accuracy," 2025. [Online]. Available: https://arxiv.org/abs/2508.00768

[25] M. Kumar, N. Singh, and B. Biswas, "Pqkelp: Projected quantum kernel embedding based link prediction in dynamic networks," *Expert Systems with Applications*, vol. 265, p. 125944, 2025. [Online]. Available: https://www.sciencedirect.com/science/article/pii/S0957417424028112

[26] J. a. P. Moutinho, A. Melo, B. Coutinho, I. A. Kovács, and Y. Omar, "Quantum link prediction in complex networks," *Phys. Rev. A*, vol. 107, p. 032605, Mar 2023. [Online]. Available: https://link.aps.org/doi/10.1103/PhysRevA.107.032605

[27] V. Bergholm, J. Izaac, M. Schuld, C. Gogolin, S. Ahmed, V. Ajith, M. S. Alam, G. Alonso-Linaje, B. AkashNarayanan, A. Asadi *et al.*, "Pennylane: Automatic differentiation of hybrid quantum-classical computations," *arXiv preprint arXiv:1811.04968*, 2018.

[28] J. Gastinger, S. Huang, M. Galkin, E. Loghmani, A. Parviz, F. Poursafaei, J. Danovitch, E. Rossi, I. Koutis, H. Stuckenschmidt, R. Rabbany, and G. Rabusseau, "Tgb 2.0: A benchmark for learning on temporal knowledge graphs and heterogeneous graphs," *Advances in Neural Information Processing Systems*, 2024.

[29] L. Yu, L. Sun, B. Du, and W. Lv, "Towards better dynamic graph learning: New architecture and unified library," *Advances in Neural Information Processing Systems*, vol. 36, pp. 67 686–67 700, 2023.

[30] R. Trivedi, M. Farajtabar, P. Biswal, and H. Zha, "Dyrep: Learning representations over dynamic graphs," in *International conference on learning representations*, 2019.

[31] Y. Wang, Y.-Y. Chang, Y. Liu, J. Leskovec, and P. Li, "Inductive representation learning in temporal networks via causal anonymous walks," *arXiv preprint arXiv:2101.05974*, 2021.

[32] Y. Luo and P. Li, "Neighborhood-aware scalable temporal network representation learning," in *Learning on Graphs Conference*. PMLR, 2022, pp. 1–1.

[33] D. Xu, C. Ruan, E. Korpeoglu, S. Kumar, and K. Achan, "Inductive representation learning on temporal graphs," *arXiv preprint arXiv:2002.07962*, 2020.